




Enhanced Upper Limb Exoskeleton Control for Stroke Rehabilitation Using Combined Electromyography and Force Sensors

Saad M. Sarhan^{1*}, Mohammed Z. Al-Faiz², Ayad M. Takhakh³

¹Department of Biomedical Engineering, College of Engineering, University of Warith Al-Anbiyaa, Karbala, Iraq

²Department of Systems Engineering, College of Information Engineering, Al-Nahrain University, Baghdad, Iraq

³Department of Mechanical Engineering, College of Engineering, Al-Nahrain University, Baghdad, Iraq

* st.saad.m.sarhan@ced.nahrainuniv.edu.iq

Article Info	Abstract
<p>Received 20/10/2024</p> <p>Revised 27/01/2026</p> <p>Accepted 27/01/2026</p>	<p>Most exoskeletons for upper limbs used in stroke rehabilitation rely solely on muscle activity signals, which are often weak and unstable. This study aimed to develop and improve the control method for these exoskeletons. Two Myo Armband sensors and six force sensors were evaluated to collect electromyography (EMG) signals and reaction forces from the forearm and upper arm regions of ten healthy participants. The data was used to control an external exoskeleton for upper limb rehabilitation, including basic hand and elbow movements. Three methodological techniques were adopted for classifying and analyzing electromyography (EMG) data: K-Nearest Neighbors (KNN), Support Vector Machine (SVM), and Linear Discriminant Analysis (LDA). Offline analysis revealed that SVM exhibited the highest accuracy, achieving an average of 95.209% for hand motions utilizing only Myo Armband data and 99.406% for elbow movements among the ten participants. A new method that uses an SVM classifier to combine EMG and force data got 99.1% accuracy. This study demonstrates the superiority of the SVM algorithm in classifying movements and enhancing control of upper limb exoskeletons.</p>
<p>Keywords: K-Nearest Neighbors; Linear Discriminant Analysis; Myo Armband; Support Vector Machine; Surface Electromyography</p>	

1. Introduction

The relationship between a human and a robot has drawn widespread interest from researchers, technology companies, and government laboratories. This has been widely harnessed to rehabilitate stroke patients [1]. Different sensing modalities, such as contact pressure sensors and finger bend, are used with EMG for controlling hand movements, which is used as a means of enabling the robotic hand exoskeletons to carry out many functions [2]. The hand and fingers are moved by a number of muscles in the arm and forearm. The deep fascia of the forearm separates the forearm into the anterior and posterior compartments. It covers 13 muscles of the forearm [3]. The anterior compartment muscles have three primary layers: the superficial layer, the intermediate layer, and the deep layer., and deep layer. The main function of these muscles is to enable the pronation of the hand as well as the flexion of the fingers and wrist. The posterior compartment muscles are found in two primary layers: the superficial layer and the deep layer. The primary function of the posterior compartment muscles is to

extend the fingers; wrist extension and supination are supplementary functions [4]. One of the distinguishing methods is believed to be systems for hand gesture recognition that rely on the identification of internal sensors (like sEMG signals)[5]. Surface electrodes and needle electrodes are the two primary electrode types used to record EMG signals (which are inserted into the skin), and they are not very different from one another [6]. There are two types of surface electrodes: gelled and dry sEMG electrodes [7]. The EMG's frequency, phase, and amplitude signals can be used to characterize it. Normally, the signal is a function of time. This signal recognizes electrical currents produced during muscle contractions, which are indicative of neuromuscular activity. Before amplification, the EMG signal's amplitude range is 0–10 mV (+5 to –5). Signals from EMG travel across different tissues and pick up noise [8]. The EMG bandwidths vary depending upon the method of study, from 0.01 Hz to 10 kHz (either invasive or noninvasive). The most important and advantageous frequency ranges are those between 50 and 150 Hz [9]. Most of the time, stroke patients' upper limb rehabilitation devices use muscle signals,

which are often weak and not very accurate. This constraint makes rehabilitation less effective. Different investigations used a robotic hand that simply used EMG data, and the overall accuracy was $77.1 \pm 5.6\%$ [10]-[12]. There is a gap in control mechanisms that needs to be filled with new ideas to make upper limb exoskeletons for stroke patient rehabilitation work better and more accurately. This research tackles the difficulty by investigating the amalgamation of advanced sensor technologies, including Myo Armband sensors and force sensors, and utilizing sophisticated classification algorithms to improve the control and precision of upper limb exoskeleton movements. The goal of this project was to make the control systems of upper limb exoskeletons used in stroke patient rehabilitation better by merging Myo Armband sensors with force sensors. The goals can be summed up like this:

- Explore the integration of two Myo Armband sensors and six force sensors to collect comprehensive data, including EMG signals and forces, from the forearm and arm regions of ten healthy subjects.
- Make an upper limb exoskeleton that is meant to help with rehabilitation, with a focus on managing movements including rest, elbow flexion and extension, hand flexion, extension, abduction, and adduction.
- Implement three distinct classification algorithms (KNN, SVM, and LDA) to analyze the collected EMG data.
- Evaluate the offline analysis results to determine the accuracy of each algorithm, with specific emphasis on the performance of SVM in classifying hand and elbow movements.

1.1 Myo Gesture Armband

The eight-channel wireless, as seen in Fig. 1, the Myo gesture control wristband is a wearable technology. For this gadget, Thalmic Labs created state-of-the-art technologies. Its three constituent parts are the gyroscope, accelerometer, and magnetometer. The Inertial Measurement Unit is represented by all of these pieces. Each of these parts represents an Inertial Measurement Unit (IMU) and has the three axes (x, y, and z) in it. There are batteries inside, and each one is in a different spot. They have a capacity of 260 mAh and a voltage range of 1.7 to 3.3 volts. It samples at a rate of 200 Hz.



Figure 1. Myo gesture armband [13]

It is also supported by the Software Development Kit (SDK), which permits connectivity with other programs like MathWorks' MATLAB [14]. The Freescale Kinetics ARM Cortex M4 120MHz MK22FN1M microcontroller unit, the

BLE NRF51822 chip, a multiprotocol Bluetooth low energy with 250 kbps, 1 Mbps, and 2 Mbps supported data rates, and an 8-bit ADC with 8 configurable channels (electrodes), are the main components integrated into the Myo gesture armband [15].

2. EMG Signal Processing

2.1 Pattern Recognition System

During the training phase, the raw EMG signal is split into segments using a pattern recognition algorithm, and feature extraction is used to turn each segment into a set of features. We use the data that these features acquire to put each segment into a group [16].

2.1.1. sEMG Segmentation

There are a number of ways to filter out the sEMG signals in the segmentation portion, including the adjacent, overlap schemes, and the segmentation approach. This study uses an overlapping approach. This method of segmentation breaks the sEMG signals into overlapping, regular time slot windows. The Classification Decision (CD) in the overlap technique can be ascertained as:

$$CD = \frac{1}{2}T_a + \frac{1}{2}T_{new} + \tau \quad (1)$$

Adjacent windowing is the term used when $T_{new}=T_a$ [17].

2.1.2 Feature Extraction and Reduction

Differentiating sEMG signal patterns requires an understanding of amplitude and frequency information. Time Domain (TD) properties relating to amplitude and frequency are useful. TD features have lately been widely exploited by academics to perform pattern identification of sEMG signals [18]. Six TD features were extracted: RMS, MAV, SSC, ZC, AR, and WL. The main objective of feature reduction is to enhance the classifier's performance. The two most widely used feature reduction methods are Principal Component Analysis (PCA) and LDA [16].

3. Classification

This study examined how successfully KNN, SVM, and LDA recognized five hand motions and two elbow movements based on sEMG data.

3.1 LDA Classifier

The purpose of LDA, like the SVM technique, is to identify a hyperplane that can divide the data points into distinct groups. If the data is normally distributed, you can find this hyperplane by finding a model that makes the distance between the class means bigger and the variation inside the class less [15]. The LDA uses Bayes' theorem for classification. For a given tested vector, x is expected to cluster with C_k , as this variance is completed in the subsequent expression:

$$P(C_k | x) = \frac{P(C_k) P(x | C_k)}{P_x} \quad (2)$$

$P(x)$ is thought to be the same for every class [19].

3.2 KNN Classifier

The KNN is an algorithm that doesn't use parameters with lazy learning. It indicates that there is no underlying data distribution hypothesis. The KNN method extends a region from the test point until it has k training samples. The test x point is then determined by applying the majority vote of these samples [16].

3.3 SVM Classifier

To implement non-linear classification boundaries, a linear model is employed. Support vector classification, which can distinguish between new sample classes, completes a computationally quick path to learning a "good" splitting hyperplane in a dimensional feature space. Depending on the separable state of the data set, several mathematical procedures are employed to generalize optimal hyperplanes [17][18]. SVM applies a nonlinear transformation utilizing suitable selection basis functions onto a higher-dimensional feature space to map the data when the situation becomes linear. The idea of applying the kernel technique is represented by this change. This study employed the Radial Basis Function (RBF) kernel as delineated in Equation (3) and a linear kernel as specified in Equation (4):

$$K(x_n, x_i) = \exp(-\gamma \|x_n - x_i\|^2 + C) \quad (3)$$

$$K(x_n, x_i) = (x_n, x_i) \quad (4)$$









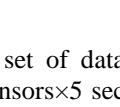
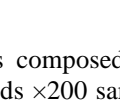
Where C , γ , and r represent the cost, gamma, and coefficient, respectively [19],[20].

4. Materials and Methods

4.1 Participants

Ten fit participants were involved in this study. Operating the Myo gesture armband, the right hand's sEMG signals were captured. Eight datasets (each containing five motions) were obtained for every individual by applying the armband on the forearm and arm regions, as indicated in Table 1.

Table 1. Hand motions based on property (Myo bands on the arm and forearm)

No.	Forearm	Arm	Name
1			rest
2			flexion
3			extension
4			adduction
5			abduction

Every single set of data is composed of 40000 samples (5 gestures×8 sensors×5 seconds ×200 samples) represented in a

5000 × 8 matrix. Furthermore, every gesture consists of 1000 data samples; the first gesture, known as rest, begins at sequence 1 and ends at 1000, the second gesture, known as flexion, begins at 1001 and ends at 2000, and so on; the fifth gesture begins at 4001 and ends at 5000. The dataset contains five-second gestures, starting with a motion of the hand at rest and ending with an adduction gesture. This means that each dataset is 25 seconds long. The entire dataset recording for each subject lasts for 200 seconds. The dataset was partitioned into a training set (80%) and a testing set (20%) using a cross-validation technique. For cross-validation, the original dataset is split into k equal-sized sub-datasets at random. While the other sub-datasets are utilized as training sets, one sub-dataset is kept as the validation information for testing the model. To do cross-validation, the recorded datasets were split up into eight smaller datasets. The identical hand gestures were recorded once again, as shown in Table 1. We additionally recorded two elbow movements—extension and flexion—for ten patients. The recording procedure was repeated by positioning the sensor on the arm area for all datasets.

4.2 Data Recording and Processing

The associated five hand gestures and two elbow movements for ten subjects were immediately recorded onto a personal laptop, where they were saved. Data processing and analysis were then done using MATLAB (Version R2020a, The MathWorks, Inc.). The signal-to-noise ratio in sEMG signals is relatively low when using the Myo gesture armband, although this has no effect on the sEMG data. The offline mode was created to increase calculation accuracy and system performance. This mode has been implemented using the MATLAB R2020 application. You should always wear the Myo gesture armband so that the sensors are always in the same areas when you use it to record datasets. To prevent inconsistent readings, this problem must be considered when recording data. In this experiment, the Myo armband is worn initially on the right forearm and then on the right arm (Table 1). This is done to see how accurate the two situations are. It is worn on the right arm as well to keep track of how much the elbow joint bends and straightens. We got the sEMG data from all of the Myo armband's channels. The Myo armband sends the data it collects to the computer via Bluetooth so that it can be analyzed and processed in the MATLAB R2020 environment. The window size of the dataset is 250 ms, with an overlap of 125 ms. The result of the eight Myo channels and the six features (RMS, MAV, SSC, ZC, WL, and AR with order = 4) that are obtained for each window (segment) adds up to 48, the total number of attributes extracted across all sets and channels. The K-NN, LDA, and SVM classifiers are used to find out how accurate the system is. Additionally, four strategically placed force sensors on the forearm region, along with a Myo Armband sensor, were employed in the experiment to accurately record and analyze muscle activity and movements related to hand flexion, extension, abduction, and adduction. Two force sensors and a Myo Armband sensor were also inserted in the arm area to help figure out how the elbow bends and straightens. The sensor array was able to detect the complicated muscle contractions and forces that were happening throughout these movements. The information from the forearm and arm areas was used to control two servo motors in the hand area and one servo motor

in the elbow area. This made the control interface work smoothly and without any problems. People might replicate natural and intuitive movements by bending, straightening, moving their arms and hands away from their body, and then bringing them back together.

The integration of force sensors and Myo Armband technology has shown a promising advancement in enhancing the functionality and control of assistive devices, emphasizing prospective applications in the sectors of augmentative and rehabilitative technologies. Fig.2 shows the response of the force sensor to the applied mass.

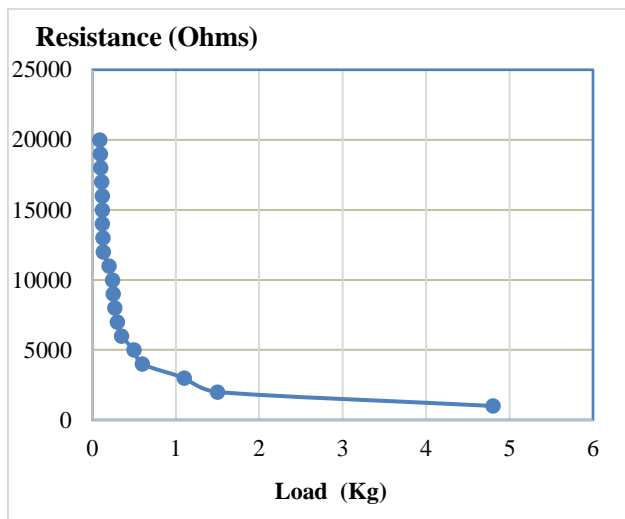


Figure 2. In the response of the force sensor, the y-axis represents the output resistance in (Ohms) and the x-axis represents the applied mass in (kg).

4.3 Mechanical Design

The exoskeleton was built utilizing a 3D printing fabrication technology. This method makes it possible to create Computer-Aided Design (CAD) models out of thermoplastics (Poly Lactic Acid (PLA)). 3D printing allows for personalization, simplicity, cost, and the use of open-source designs. It has three degrees of freedom (DOF), which are as follows:

- **Elbow Flexion/Extension:** The user's arm can be bent and straightened by the exoskeleton, simulating the flexion and extension actions, according to the servo motor located at the elbow.
- **Wrist Flexion/Extension:** A servo motor in the hand region is in charge of the flexion and extension of the wrist, which are necessary for carrying out a variety of daily chores.
- **Wrist Abduction/Adduction:** The exoskeleton can perform these movements by utilizing the second servo motor in the hand region.

Fig. 3 displays the final design and individual components.

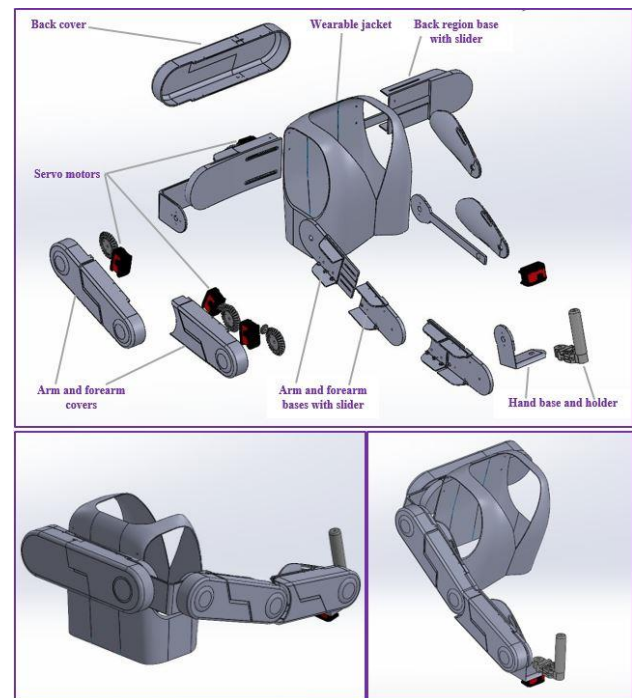


Figure 3. Shows separate components and the finished design.

5. Results and Discussions

This section examines the findings of the research and the factors affecting the accuracy of the system. Determining criteria include the classifier, the length of the window, and the type of characteristics used.

5.1 Length and accuracy of the window

The window size grew from 100 milliseconds to 700 milliseconds. The optimal results were achieved by balancing system precision and delay time, using a 250 ms window size and 125 ms overlapping, due to the fact that recognition accuracy decreased at window lengths of 260 ms or more and 240 ms or less. These values have been adopted in the online mode.

5.2 Accuracy and Features Extracted

Eight channels and six features were chosen for the 10 participants. Out of all the features of MAV, RMS, WL, AR, ZC, and SSC, ZC had the least effect on accuracy. The SVM classifier, with an average value of 95.209% in offline mode, was used to achieve the best accuracy.

5.3 Channels Number

Fig. 4 shows the seven moves that use eight channels of the Myo armband with 1000 samples (5 sec.) for every movement listed in the order rest, flexion, extension, abduction, adduction, elbow flexion, and extension.

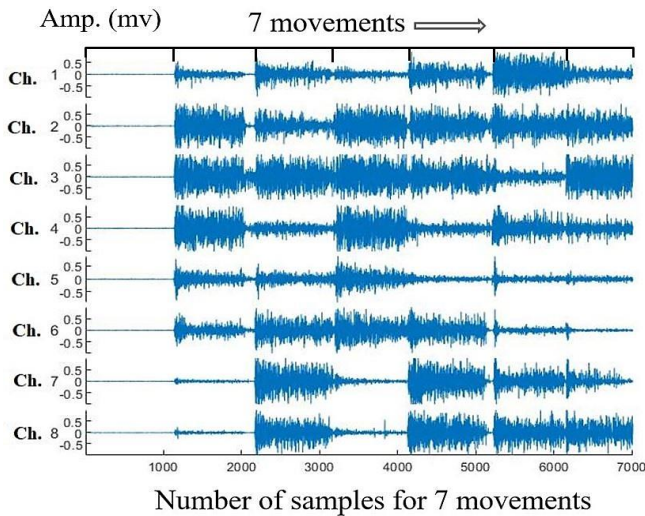


Figure 4. Eight channels were used to record the raw EMG data for seven motions

The amplitude of each sensor changes with each movement because of where the electrodes are placed on the forearm. Channel 5 doesn't affect the accuracy of the categorization; thus, it can be left out of the measurement to cut down on the quantity of data. Fig. 5 presents the average recognition accuracies (%) when 8 sensors are used, and the Myo armband is put on the forearm.

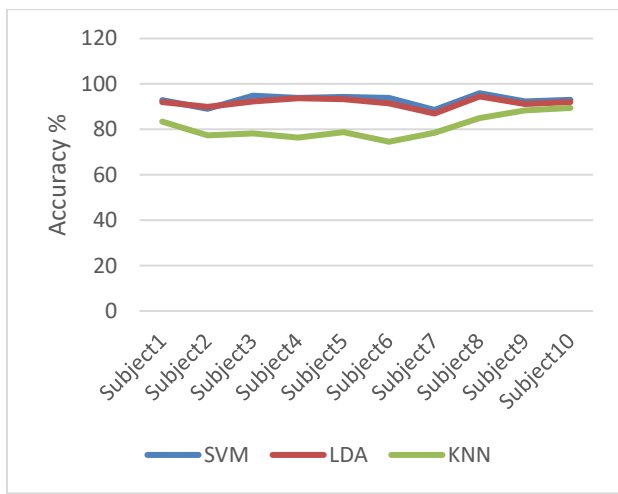


Figure 5. Average recognition accuracies when wearing the Myo Armband on the forearm.

The SVM classifier outperformed the LDA and KNN classifiers in terms of classification accuracy, as seen in Fig. 5. This process was repeated by putting the sensor on the arm, which shows that the SVM is the best classifier according to these results. For ten patients, the average SVM accuracies were 61.904% for the arm region and 95.209% for the forearm region. The forearm's 33.305% hand movement result was superior to the arm's. By putting the sensor in the arm area, as shown in Fig. 6 below, the elbow flexion and extension were also recorded (%).

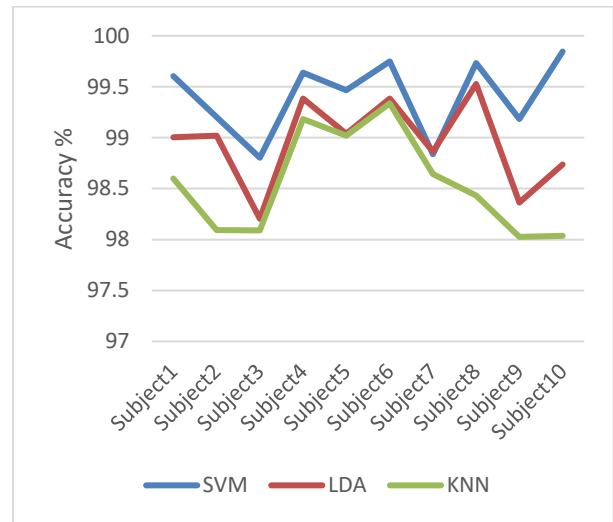


Figure 6. Average recognition accuracies when placing the sensor on the arm region.

The SVM outperformed the other two classifiers, as the aforementioned results demonstrate. Two factors contribute to the high categorization accuracy of elbow movements: first, there are just two actions (flexion and extension); second, the muscles that perform these two movements are located in non-overlapping locations (triceps for extension and biceps for flexion).

5.4 Fusion of Myo Armband and Force Sensors

The combination of six strategically placed force sensors on the forearm and arm with the Myo armband has shown to be a strong way to control the movements of an upper limb exoskeleton. The four force sensors on the forearm pick up muscle activity and force exertion throughout different movements. This gives important information about what the user wants to do. In addition, the two force sensors on the arms give important information about the forces applied to the arms. The Myo armband improves the control system by getting electrical signals from the user's muscles and turning them into specific movement commands, as seen in Fig. 7. This network of different types of sensors makes sure that the exoskeleton always understands what the user is doing, so it can easily imitate and improve what they do. The fusion makes the control more precise and responsive, which makes it easier and faster to use the exoskeleton. An SVM classifier was used to test the suggested strategy. It got 99.1% accuracy by combining EMG and force data. This new strategy, which employs technology to make neuroplasticity better, retrain motor abilities, and improve recovery results, could make stroke therapy more personalized and successful.

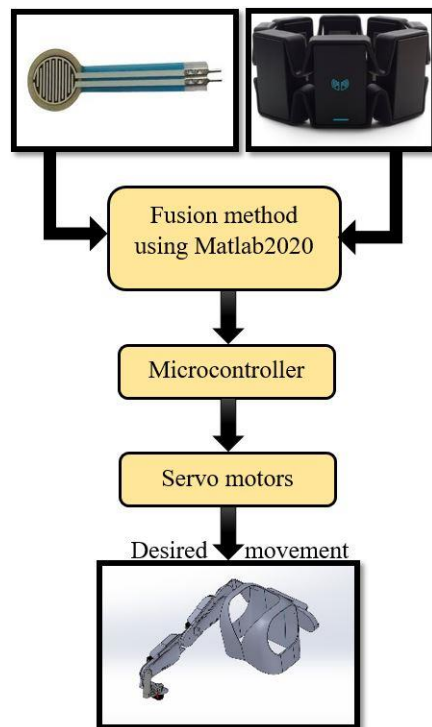


Figure 7. Final block diagram.

6. Conclusion

The goal of this work was to improve the control systems of upper-body exoskeletons used in stroke rehabilitation by combining the Myo Armband sensor with force sensors. Using an SVM classifier was highly precise, getting 99.406% of elbow movements right. SVM's use of both EMG and force data was new and very accurate, with an accuracy rate of 99.1%. This approach might transform how people get their motor abilities back after a stroke. SVM's higher performance suggests that it could be utilized to make individualized and successful programs for rehabilitation. The results demonstrated that the size of the window has a considerable impact on how well the system works. The online test demonstrated that the Myo Armband and force sensors worked well together, which made it easy to control the exoskeleton. For future research in this field, it would be beneficial to obtain additional data from both individuals with disabilities and those without. This would help us figure out how accurate the system is more clearly.

The purpose of this study was to enhance the control systems of upper-body exoskeletons utilized in stroke therapy by integrating the Myo Armband sensor with force sensors. It was very accurate to use an SVM classifier, which got 99.406% of elbow movements accurately. It was new and very accurate for SVM to use both EMG and force data. It had an accuracy rate of 99.1%. This method could change how people recover their motor skills after a stroke. Because SVM works better, it might be able to design personalized and effective rehabilitation regimens. The results showed that the size of the window has a big effect on how well the system functions. The online test showed that the Myo Armband and force sensors worked well

together, which made it easy to control the exoskeleton. For future research in this domain, it would be advantageous to gather supplementary data from both those with disabilities and those without. This would let us better understand how accurate the system is.

Abbreviations

T_a	The analytical window's length
T_{new}	The increase in the window
τ	The processing time
$P(x C_k)$	The test vector's probability density function in the k class
$P(C_k)$	The prior probability
$P(x)$	The probability density function of the training space
C	Cost of the penalty
γ	Gamma
r	Coefficient

Conflict of interest

The authors affirm that there are no competing interests concerning this manuscript's publication.

Author Contribution Statement

Saad M. Sarhan and Mohammed Z. Al-Faiz: technique and formal analysis.

Saad M. Sarhan: software, composing the first draft, and resources.

Ayad M. Takhakh: getting money, checking things, making things look good, and running projects.

Mohammed Z. Al-Faiz: looking into things, organizing data, producing reviews and edits, and keeping an eye on things.

References

- [1] E. Schneiders, "Non-dyadic human-robot interaction: Concepts and interaction techniques," in *2022 17th ACM/IEEE International Conference on Human-Robot Interaction (HRI)*, Mar. 2022. doi: <https://doi.org/10.1109/HRI53351.2022.9889463>
- [2] S. Hall and J. Stephens, *Anatomy and Physiology*, 5th ed. Amsterdam, Netherlands: Elsevier, 2019.
- [3] M. T. Duruöz, Ed., *Hand Function: A Practical Guide to Assessment*, 2nd ed. Istanbul, Turkey: Springer, 2020.
- [4] S. Bisi, L. De Luca, B. Shrestha, Z. Yang, and V. Gandhi, "Development of an EMG-controlled mobile robot," *Robotics*, vol. 7, no. 3, p. 36, Jul. 2018. doi: <https://doi.org/10.3390/robotics7030036>
- [5] O. Ülker, G. Gö, and E. Kaplanoglu, "EMG signal classification using fuzzy logic," *Balkan Journal of Electrical and Computer Engineering*, vol. 5, no. 2, pp. 97–101, 2017. doi: <https://doi.org/10.17694/bajece.337941>
- [6] M. A. Ozdemir, D. H. Kisa, O. Guren, and A. Akan, "Dataset for multi-channel surface electromyography (SEMG) signals of hand gestures," *Data in Brief*, vol. 41, p. 107921, Apr. 2022. doi: <https://doi.org/10.1016/j.dib.2022.107921>
- [7] Z. H. Zaier and K. K. Resan, "Effect of the gait speed on a new prosthetic shank below knee," *Journal of Engineering and Sustainable Development*,

- vol. 26, no. 4, pp. 63–69, Jul. 2022. doi: <https://doi.org/10.31272/jeasd.26.4.7>
- [8] P. K. Koppolu and K. Chemmangat, “A comparison of different signal processing techniques for upper limb muscle activity onset detection using surface electromyography,” 2023 3rd International Conference on Artificial Intelligence and Signal Processing (AISP), Mar. 2023. doi: <https://doi.org/10.1109/aisp57993.2023.10134857>
- [9] P. J. Gonzalo and J. A. Holgado-Terriza, “Control of home devices based on hand gestures,” in *2015 IEEE 5th International Conference on Consumer Electronics - Berlin (ICCE-Berlin)*, pp. 510–514, 2016. doi: <https://doi.org/10.1109/ICCE-Berlin.2015.7391325>
- [10] E. Kaya and T. Kumbasar, “Hand gesture recognition systems with the wearable Myo armband,” in *2018 6th International Conference on Control Engineering & Information Technology (CEIT)*, Oct. 2018. doi: <https://doi.org/10.1109/CEIT.2018.8751927>
- [11] P. Visconti, F. Gaetani, G. A. Zappatore, and P. Primiceri, “Technical features and functionalities of Myo armband: An overview on related literature and advanced applications of myoelectric armbands mainly focused on arm prostheses,” *International Journal on Smart Sensing and Intelligent Systems*, vol. 11, no. 1, pp. 1–25, 2018. doi: <https://doi.org/10.21307/ijssis-2018-005>
- [12] J. P. Mueller and L. Massaron, *Machine Learning for Dummies*, 2nd ed. Hoboken, NJ: John Wiley et Sons, Inc, 2021.
- [13] H. Bengacemi, A. Gharbi, P. Ravier, K. Abed-Meraim, and O. Buttelli, “Surface EMG signal segmentation and classification for Parkinson’s disease based on HMM modelling,” in *Proceedings of the 13th International Conference on Pattern Recognition Applications and Methods*, 2024. doi: <https://doi.org/10.5220/0012572900003654>
- [14] A. H. Shah, A. H. Miry, and T. M. Salman, “Automatic modulation classification using Deep Learning Polar Feature,” *Journal of Engineering and Sustainable Development*, vol. 27, no. 4, pp. 477–486, Jul. 2023. doi: <https://doi.org/10.31272/jeasd.27.4.5>
- [15] A. Chaudhary, “Introduction,” in *Robust Hand Gesture Recognition for Robotic Hand Control*, pp. 1–5, Jun. 2017. doi: https://doi.org/10.1007/978-981-10-4798-5_1
- [16] A. Furui, “Evaluating classifier confidence for surface EMG pattern recognition,” in *2023 45th Annual International Conference of the IEEE Engineering in Medicine & Biology Society (EMBC)*, Jul. 2023. doi: <https://doi.org/10.1109/EMBC40787.2023.10340977>
- [17] S. Abdulwahab, H. Khleaf, and M. Jassim, “EEG Motor-Imagery BCI System Based on Maximum Overlap Discrete Wavelet Transform (MODWT) and Machine Learning Algorithm,” *Iraqi Journal for Electrical and Electronic Engineering*, vol. 17, no. 2, pp. 38–45, Jul. 2021, doi: <https://doi.org/10.37917/ijeee.17.2.5>.
- S. M. Sarhan, M. Z. Al-Faiz, and A. M. Takhakh, “A review on EMG/EEG based control scheme of upper limb rehabilitation robots for stroke patients,” *Heliyon*, vol. 9, no. 8, p. e18308, 2023. doi: <https://doi.org/10.1016/j.heliyon.2023.e18308>
- [19] A. F. Rochim, K. Widyaningrum, and D. Eridani, “Performance comparison of support vector machine kernel functions in classifying COVID-19 sentiment,” in *2021 4th International Seminar on Research of Information Technology and Intelligent Systems (ISRITI)*, Dec. 2021. doi: <https://doi.org/10.1109/ISRITI54043.2021.9702845>
- [20] Saad M. Sarhan, M. Z. Al-Faiz, and A. Takhakh, “EEG-based control of a 3D-printed upper limb exoskeleton for stroke rehabilitation,” *International Journal of Online and Biomedical Engineering (iJOE)*, vol. 20, no. 09, pp. 99–112, Jun. 2024. doi: <https://doi.org/10.3991/ijoe.v20i09.48475>